Thermal Optimisation of *1.3μm dilute nitride lasers* Chapter 6

6.1 Introduction

The reliability and lifetime of a device is strongly dependent upon its operating temperature. Indeed, elevated temperatures are commonly used in accelerated device aging tests [1,2]. As a rule of thumb, for every 10K increase in operating temperature, the device lifetime decreases by a factor of two [3]. Thus, it is essential that a device be optimized thermally as well as electronically and optically. In this chapter, the results from a series of simulations are presented, which were carried out to optimise the thermal performance of the passively cooled 1.3μm dilute nitride lasers. The devices modeled were based on the same epitaxy as those studied in Chapters 3-4. The model developed in Chapter 5 was used to perform full opto-electro-thermal simulations of these devices.

6.2 The device and its thermal performance

The device simulated was 300μm long and had a stripe width of 3.2μm. The power reflectivities of the front and back facets were 0.3 and 0.7, respectively. It is usual to mount the device p-side up, so that the ridge can be easily contacted with a coplanar probe and a high modulation rate achieved. Figures 6.1 and 6.2 show the two main forms in which the 1.3μm devices were produced. Figure 6.1 shows a simple RW structure. The ridge can be seen in the center of the image and a thin layer of gold can be seen covering the top of the device. Figure 6.2 shows a device processed

specifically to achieve a high frequency modulation response. The same RW structure as shown in figure 6.1 is visible in the center the image. However, in this device, a large area mesa structure has been formed by etching down to the n^+-GaAs substrate and the entire structure can be seen to be covered by a thick layer of BCB. This process reduces the total device capacitance and thus improves it's modulation response. In this image, the gold contact metal has not yet been deposited.

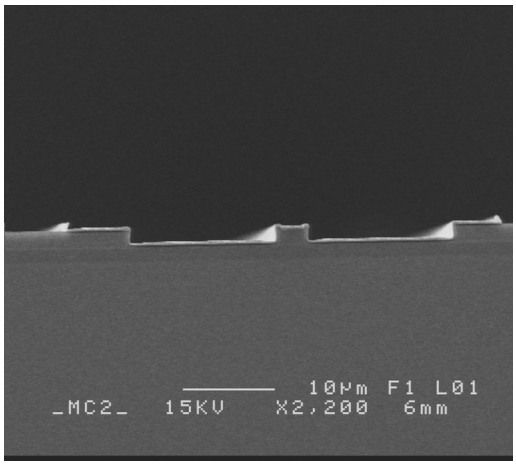

Figure 6.1: SEM image of the standard RW structure. Courtesy of Chalmers University of Technology, Sweden.

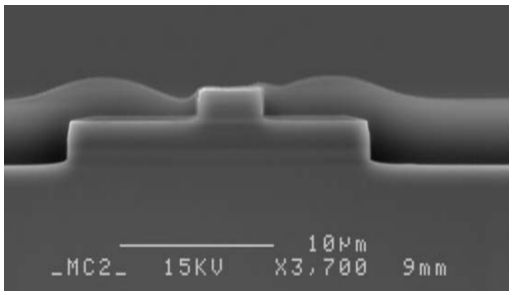

Figure 6.2: SEM image of the high modulation response RW structure before metalisation. The wide area mesa structure is visible in the image. Courtesy of Chalmers University of Technology, Sweden.

There is a great deal of heating in the RW structure. All of the current flowing into the device must first pass through the narrow ridge structure, generating Joule heat. Also, a large proportion of the optical mode is confined within the RW leading to

large amounts of free carrier absorption. The ridge waveguide is very close to the QW, so any change in ridge temperature will lead to a significant change in the QW temperature, and hence reduce the gain and device performance.

Figure 6.3a shows a high magnification image of the RW structure shown in figure 6.1. Figure 6.3b shows the typical thermal conductivity profile associated with the RW. The for main features in the image are the double stripes of the QW, the ridge, the gold top contact of high conductivity and the etched trench of very low thermal conductivity.

Depending upon how gold is deposited on the ridge, the thermal properties of the ridge can be significantly altered. If, as in figure 6.1, gold is evaporated onto the ridge, down its sides and along the etched trench, the laser's thermal performance is greatly improved. This is because the high conductivity of the gold allows heat to easily escape the ridge and the vicinity QWs.

In the structure optimised for high speed modulation, BCB, a polymer with a very low thermal conductivity, separates the gold top contact from the sides of the ridge waveguide – thus reducing device capacitance. However, this also prevents heat from flowing out of the sides of the ridge. The gold top contact also never touches the substrate, thus heat cannot conduct away through the top of the ridge. Any heat generated in the ridge can only escape through the bottom of the ridge. This reduces the overall thermal performance of the structure. In the remainder of the chapter, the

thermal performance of these two structures will be systematically investigated.

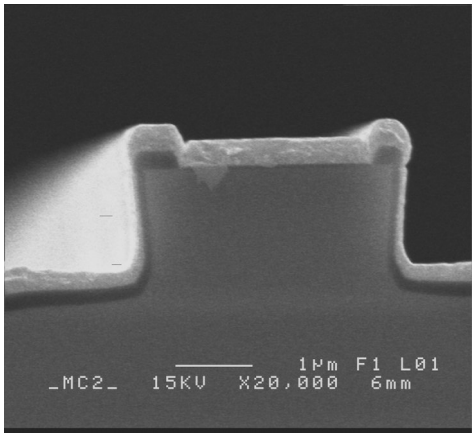

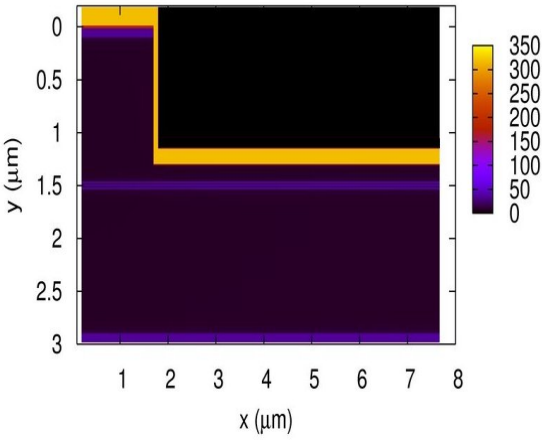

Figure 6.3a: High magnification image of the RW structure. Courtesy of Chalmers University Sweden.

Figure 6.3b: Plot of thermal conductivity ($Wm^{-1}k^{-1}$) of RW structure.

6.3 Comparison with experiment

The thermally dependent device simulator developed in Chapter 5 was calibrated with known data from Chalmers University of Technology and Modulight Inc. A comparison of the simulated and experimental LI-curves for the ordinary RW structure is shown in figure 6.4. A comparison of the simulated and measured QW temperature from chapter 4 is shown in figure 6.5. Although only the LI curves were used in calibrating the model, relatively good agreement is obtained in terms of the QW temperature.

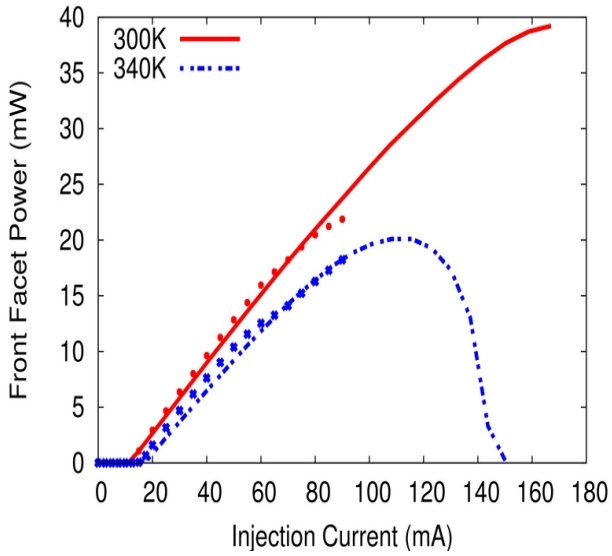

Figure 6.4: Simulated and experimental LI curves. The dotted curves are experimental.

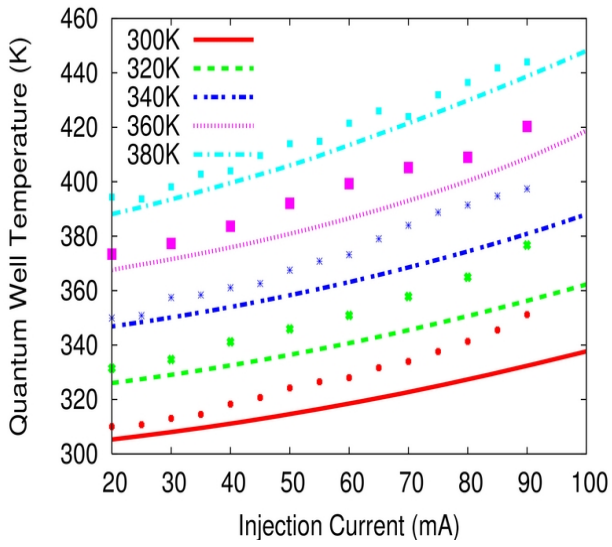

Figure 6.5: Simulated and experimental QW temperatures.

6.4 Thermal comparison of the mesa and ordinary RW structures

In figure 6.6, the temperature performance of the mesa and ordinary RW structure is plotted. It can be seen that the ordinary RW out performs the mesa structure in terms of active region temperature. The reason for this can be found by examining the SEM images in figures 6.1 and 6.2. In the ordinary RW structure, there is a layer of gold across the entire top of the device, which helps spread heat away from the ridge and reduces the active region temperature. In the high-speed structure, the gold layer is separated from the device by a thick insulating layer of BCB, so that any heat generated in the ridge must flow down through both the ridge RW and the QWs.

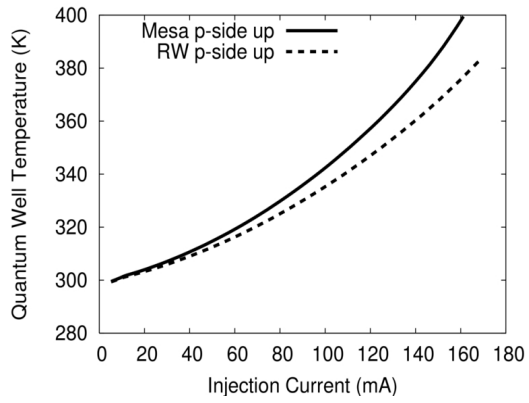

Figure 6.6: Simulated QW temperature of the mesa and ordinary RW structure.

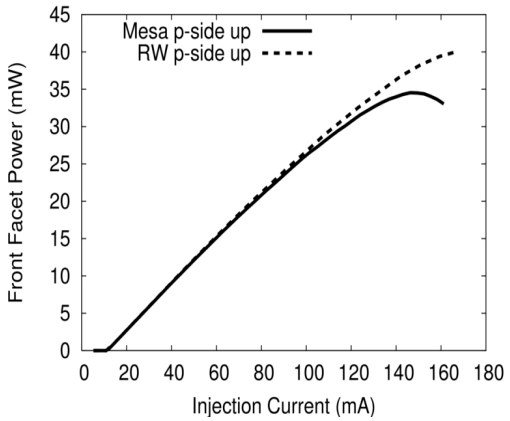

Figure 6.7: Simulated LI curves of the RW structure and the mesa structure.

Figure 6.7 plots the corresponding simulated LI curve for the devices. Although the only major change in the device structure is the insertion of the BCB layer between the gold and the device, this results in the early onset of thermally induced roll over.

6.5 Filled etched trenches with gold straight across

If figure 6.3a is examined, one of the most interesting features from a thermal point of view is the gold contact. It is highly conducting and can rapidly transport heat away from the ridge. Notably, due to the deposition process, there is a thinner layer of gold on the vertical sides of the RW than on the top. In this section, the thickness of the gold in four areas will be varied to examine the impact on the thermal performance. These areas are on either side of the etched trench, on the bottom of the etched trench and the horizontal layer on top of the device. A schematic of the regions that will be varied is shown in figure 6.8.

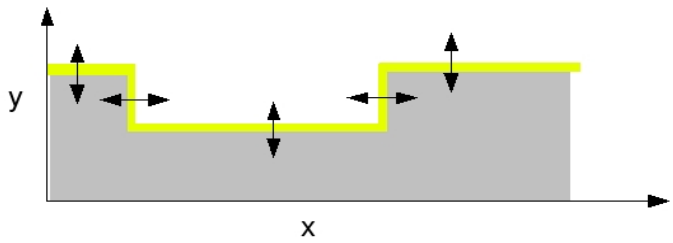

Figure 6.8: Schematic of the RW/etched trench and the covering layer of gold.

6.5.1 Variation of gold on the side of ridge

In figure 6.3a, the layer of gold on the left hand side of the RW structure can be seen to be slightly thinner than that on the rest of the contact. This could decrease heat flow down the ridge and thus affect the QW temperature. Figure 6.9 shows the results from simulations where the thickness of this layer has been varied from 0μm to 0.4μm. It can be seen that the thickness of the gold layer has very little impact on the QW temperature.

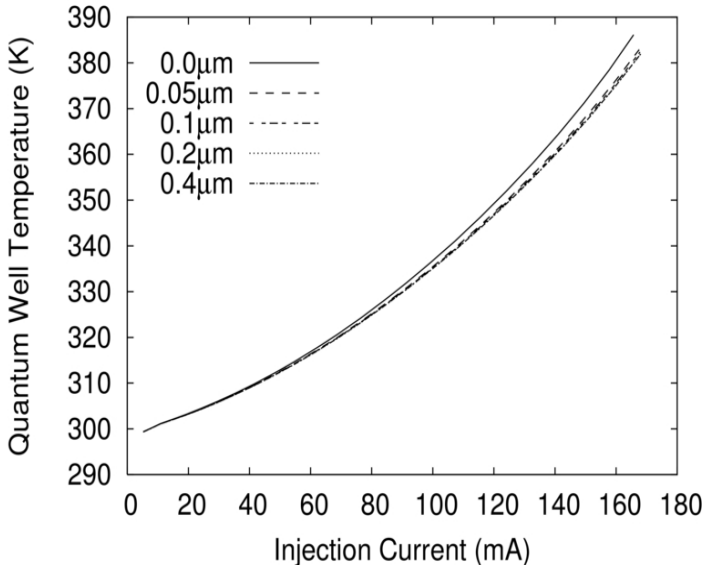

Figure 6.9: The impact of varying the thickness of the gold on the side of the ridge.

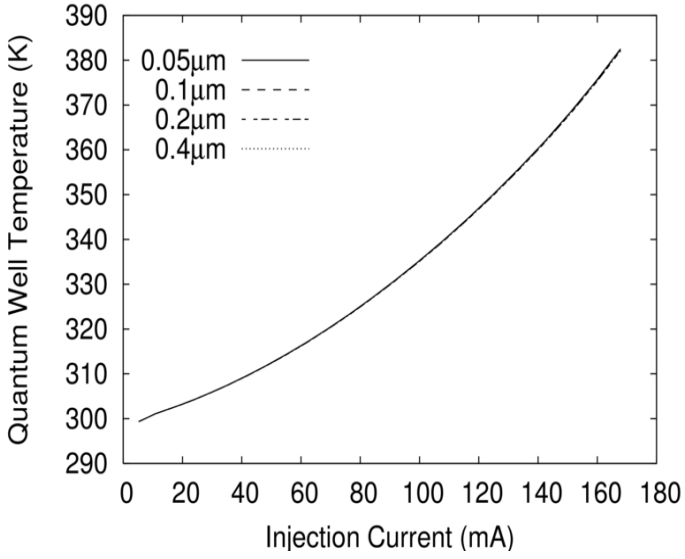

Figure 6.10: Variation of thickness of gold on the far side of the trench.

At very high injection currents, there is a 5K difference in QW temperature between simulations with a thick layer of gold deposited and having no gold deposited. For completeness, the thickness of gold was varied on the far side of the etched trench. Figure 6.10 shows that this had no impact on the QW temperature.

6.5.2 Variation of gold on the bottom of trench

A great deal of heat is generated around and under the ridge waveguide. The thickness of the layer of gold on the bottom of the etched trench was varied to examine if this helped channel heat out of the structure.

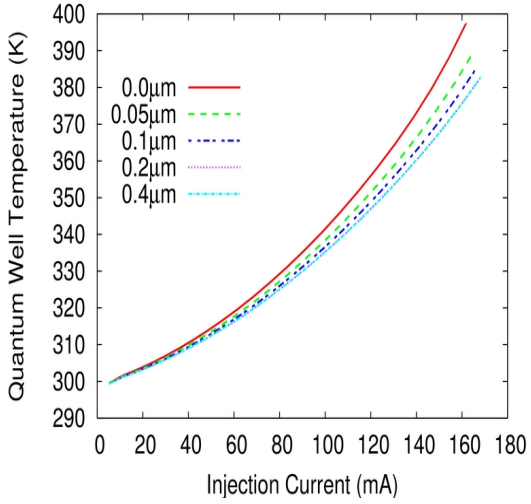

Figure 6.11: Variation of thickness of gold on the bottom of the etched trench.

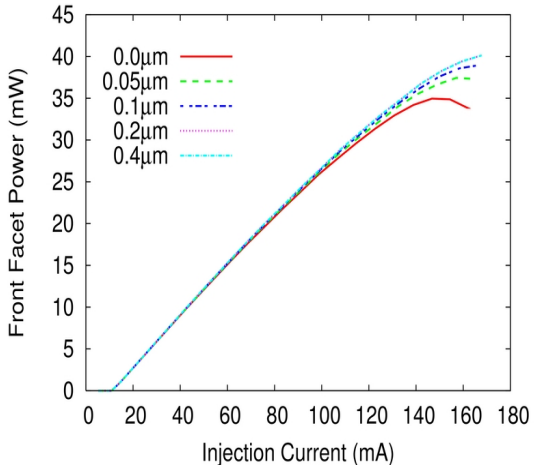

Figure 6.12: LI curve corresponding with varying thickness of gold on the bottom of the etched trench.

At high injection currents, a difference between having no gold and having a thick layer of gold gives a 20K difference in QW temperature (see figure 6.11). The layer of gold the bottom of the etched trench clearly contributes to the effective channeling of heat out of the RW structure. The corresponding set of LI curves is plotted in figure 6.12. At very high injection currents, an increased thickness in the layer of gold can delay the onset of thermally induced roll-over.

6.5.3 Variation of gold on the top of the device

The thickness of gold on the top of the device was varied. This included the ridge and the outlying region of gold past the RW structure. The thickness of this layer was found to have a very small impact on the thermal performance of the device (see figure 6.13).

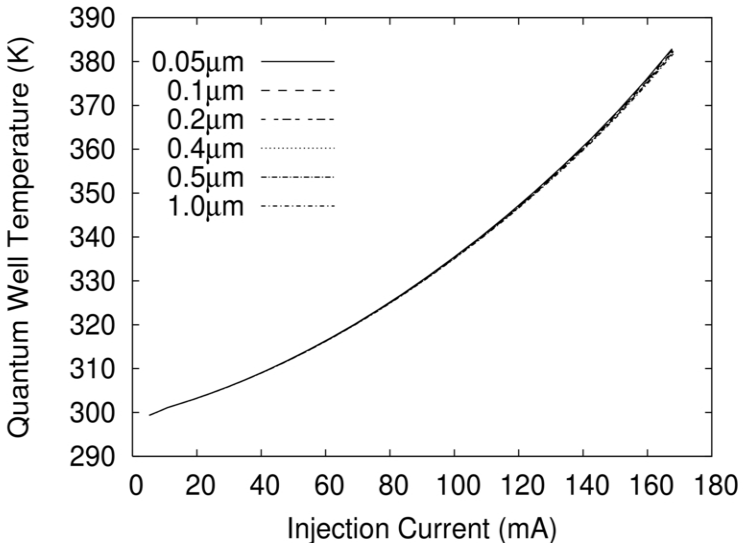

Figure 6.13: Variation of gold deposited on the top contact of the device (not in the etched trench).

6.6 Mounting the device p-side up or p-side down

Packaging costs are reduced by mounting a device p-side up. However, there is a significant thermal penalty for mounting the device in this way. The devices are grown on top of a 300-500μm GaAs substrate, which is then thinned to 100μm. When mounted p-side up, the active region is separated from the heat sink by this substrate, resulting in a very high effective thermal resistance and raising the device temperature. Conversely, if the device is mounted p-side down, the heat can escape straight into the heat sink, which has a very high thermal conductivity. This reduces the active region temperature. In this section, the impact of p-side up mounting of both structures, RW optimised for high modulation response and the ordinary RW structure, are examined. Figure 6.14 plots the simulated injection current versus active region temperature for the ordinary RW structure mounted p-side up and p-side down. The difference in thermal performance between devices mounted p-side up and p-side down is dramatic, with the p-side up device becoming up to 70K hotter at high injection currents. The corresponding simulated LI curves are shown in figure 6.15. Unlike the p-side up device, the p-side down mounted device experiences almost no roll-over.

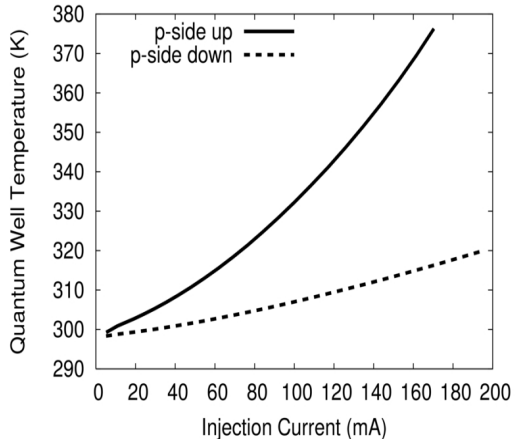

Figure 6.14: Simulated quantum well temperature for the low modulation speed device versus injection current.

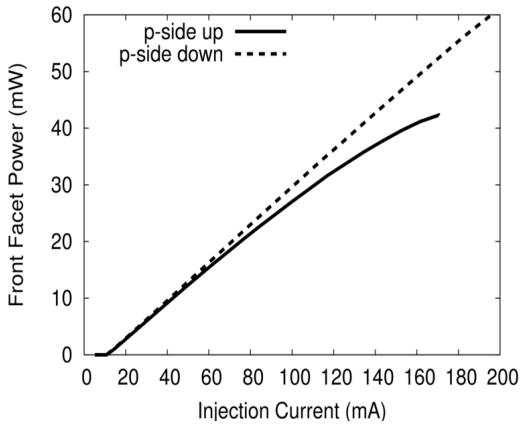

Figure 6.15: The simulated LI curve for a p-side up/down mounted device.

For the large area mesa structure, the p-side up device also performs worse than the p-side down mounted device and figure 6.17 shows an even more rapid onset of thermally induced roll-over.

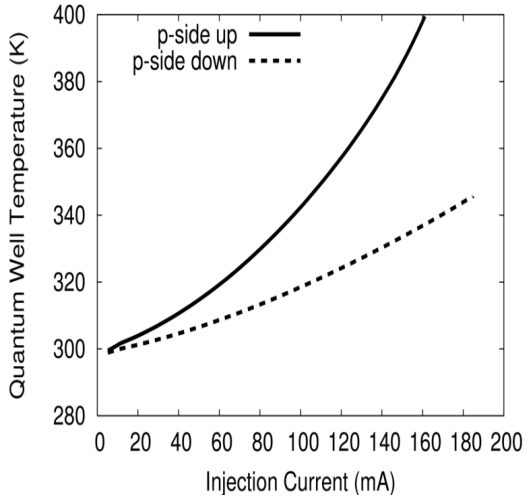

Figure 6.16: Simulated QW temperature of the structure optimised for a high modulation response mounted p-side up and p-side down.

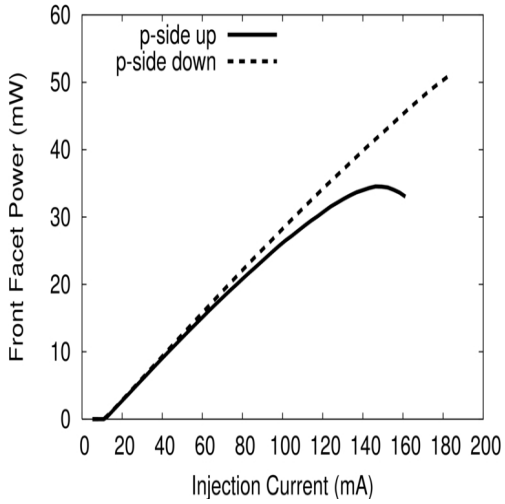

Figure 6.17: Simulated LI curves of the structure optimised for a high modulation response mounted p-side up and p-side down.

6.7 Mesa p-side up/down mounting at elevated temperatures

The dilute nitride laser described in this work is aimed at the access network market, where active cooling is undesirable because it pushes up the unit cost. Therefore, it is likely that the heat sink temperature will rise to well above the ambient temperature. To assess the possible benefit of p-side down mounting at elevated temperatures, the simulations in the previous section were performed again at heat sink temperatures of 300K, 320K, 340K, 360K and 380K. One set of simulations was performed with the mesa structure mounted p-side up and one with the mesa structure mounted p-side down. The results are shown in figures 6.18 and 6.19. As the external temperature of the heat sink rises, mounting p-side up has a larger impact on the temperature of the

active region. It can be seen that for the p-side up mounted devices the QW can reach temperatures as high as 400K, when the external heat sink temperatures rise above 320K. At a heat sink temperature of 380K, a decrease in QW temperature of 25K is obtained by mounting p-side down. Although it is hard to predict lifetimes from such data, a rule of thumb commonly used is that for every ten degrees decrease in active region temperature, the device lifetime doubles [1,2]. This would suggest that by mounting the devices p-side down a lifetime up to 2.5 times longer could be achieved.

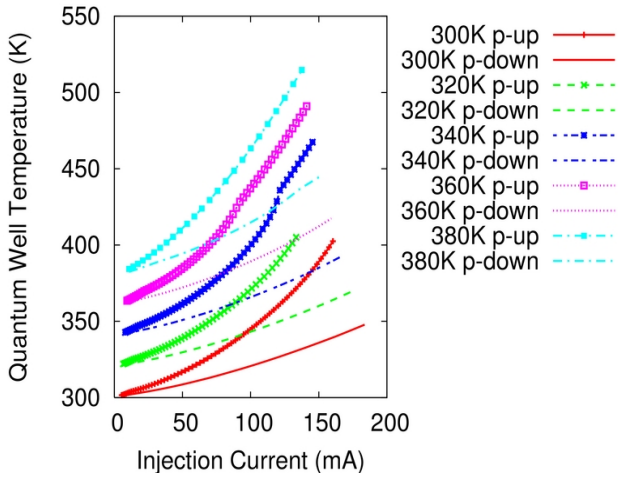

Figure 6.18: Simulated temperature profile of device at elevated temperatures.

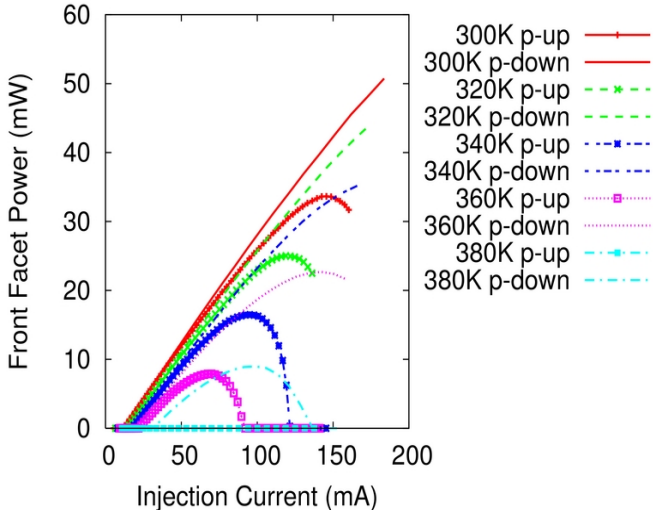

Figure 6.19: Simulated LI curve of device at elevated temperatures.

6.8 Impact of substrate height on maximum temperature

It is possible to reduce the thermal resistance of the substrate by post growth substrate thinning. A series of simulations were performed considering the effect a thinned substrate would have. This is shown in figure 6.20 and the corresponding LI curves are shown in figure 6.21. It can be seen that the substrate thickness significantly impacts the thermal performance of the p-side up device. This suggests that thinning the substrate could potentially achieve a large decrease in temperature and with it a large increase in device reliability.

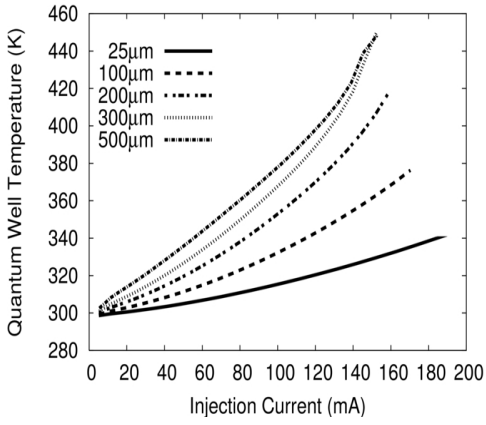

Figure 6.20: Impact of substrate thickness on device temperature.

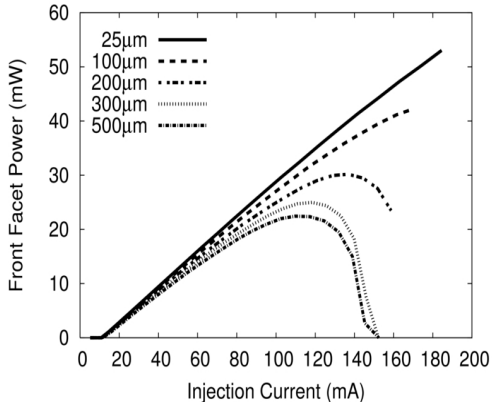

Figure 6.21: Impact of increased substrate thickness on LI curve.

6.9 Etch depth of large area mesa structure in the high modulation frequency device

The large area mesa structure of the high speed RW device is defined by etching back

the epitaxy to the n-type substrate. The thermal conductivity of the mesa structure is plotted in figure 6.22. The RW and mesa structure is then covered with a layer of BCB before a top contact of gold is applied. The depth of the etch used to define the mesa structure is a variable. In this section, a set of simulations were performed to determine the impact of etch depth on the device performance. The mesa depth was varied, from 0μm (i.e. no etching at all), to an etch depth of 16μm. This distance is shown in figure 6.22 by the arrow marked with a *.

The results are presented in figure 6.23. It can be seen from the figure that generally the etch depth has very little impact on the QW temperature. This suggests that lateral heat flow within the substrate far away from the ridge is unimportant. However, as soon as the mesa etch depth reaches 0μm, so that the top contact is connected to the epitaxy, a sudden decrease in QW temperature is seen. The reason for this is that a secondary heat flux path out of the ridge has been introduced from the ridge through the top contact and to the substrate.

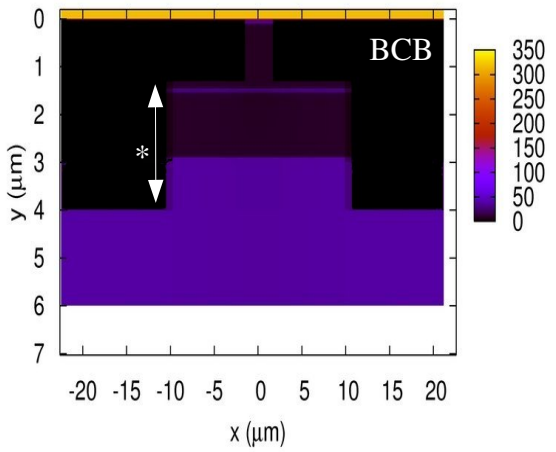

*Figure 6.22: Thermal conductivity of the mesa structure. *Mesa etch depth.*

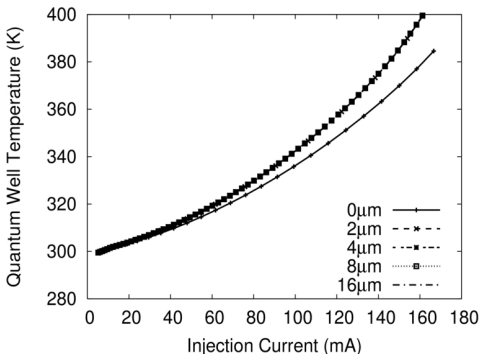

Figure 6.23: QW temperature for various mesa etch depths against injection current.

6.10 Thermal conductivity of the etched trench

In section 6.4, it was shown that conducting heat away from the ridge as quickly as possible is essential if low operating temperatures are to be achieved. One way to remove heat from the ridge region is to refill the etched trenches with something more thermally conductive than BCB. To investigate this, materials with different thermal conductivities were considered - all of which had a relatively low refractive index/permittivity (see table 6.1).

Material	***k*** **($Wm^{-1}K^{-1}$)**	***n***	ε_r
SiO_2	1.36 [4]	1.46	1.2
Al_2O_3	25.12 [4]	1.5	1.22
Si_3N_4	30.14 [4]	2.05	1.431
BCB Benzo-cyclobutene	0.29 [5]	1.54 [5]	1.24

Table 6.1: Material phonon thermal conductivities considered during the investigation.

Figures 6.24 and 6.25 show the thermal impact of filling the etched trenches for the p-side up mounted mesa structure. At very high injection levels, a small (~2-3K) decrease in QW temperature is observed due to the replacement of the BCB by a substance with higher thermal conductivity.

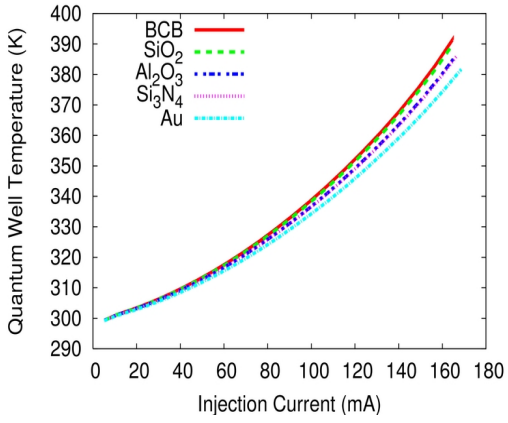

Figure 6.24: QW temperature of the mesa structure for various etch trench fillings at 300K.

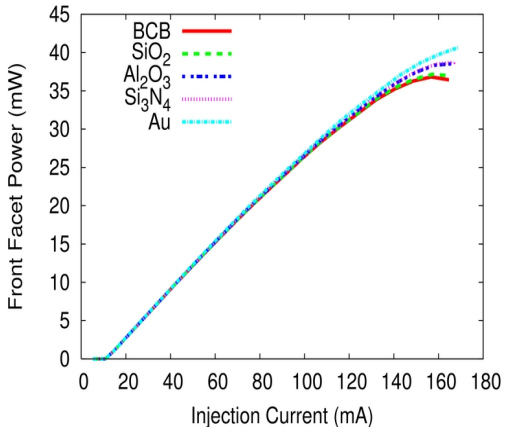

Figure 6.25: LI curve of the mesa structure for various etch trench fillings at 300K.

The impact of the change in temperature can be seen in the L-I curve in figure 6.25.

In fact, there is very little impact to the L-I curve, for typical operating conditions (10-15mW), but a small difference is seen in the roll over region. However, at higher temperatures, the situation is different. Figure 6.26 shows a plot of the QW temperature for a heat sink temperature of 360K. The corresponding dramatic change in the LI curve is shown in figure 6.27. At high temperatures, considerably more heat is being generated due to the lower carrier mobilities and higher dark recombination rates, so that using a different material to refill around the ridge could have a significant impact on the device lifetime and performance.

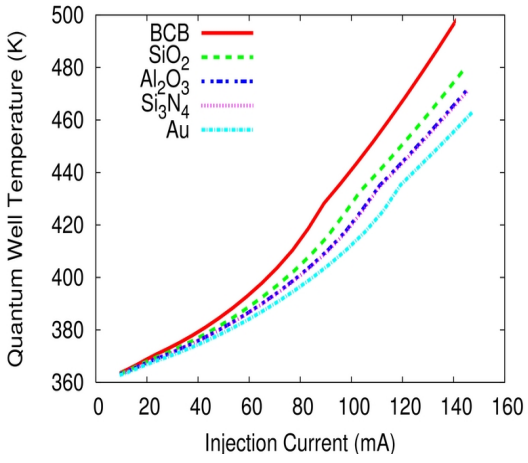

Figure 6.26: p-side up mounted device at 360K.

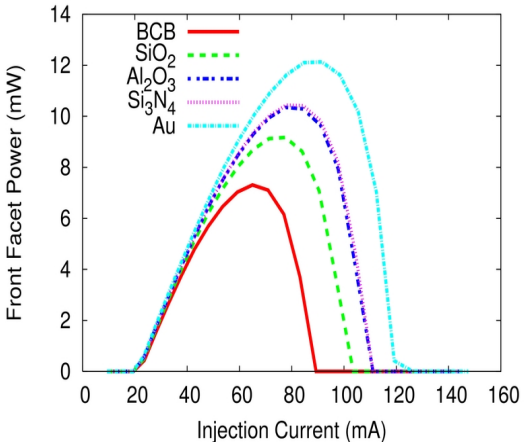

Figure 6.27: p-side up LI-curve for various trench fillings at 360K.

6.11 Using a small stub to extract heat from the top of the ridge

In the above simulations, it has been established that the thermal conductivity of the

etched trench can significantly alter the thermal performance of the device. Refilling the etch trench is technologically difficult and introduces another process step. For both these reasons, it could be considered undesirable. It would be desirable if another heat flux path could be introduced to extract heat from the top of the ridge in a technologically easy manner.

An alternative to refilling the etched trench would be to connect the top of the RW, thermally (but not electrically) to the substrate. If during the etching of the RW structure, another smaller ridge were etched some way away from the RW and covered with a passivating layer to prevent electrical conduction, then after gold had been deposited onto the device, it could act as a secondary heat flux path, drawing heat away from the ridge and the active region. Such a situation is depicted in figure 6.28.

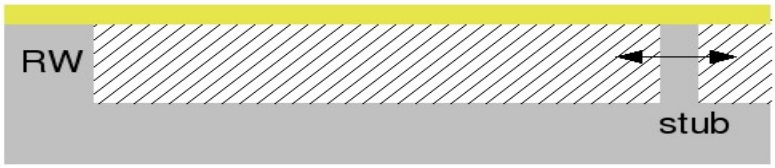

Figure 6.28: Introducing a small stub into the epitaxy to help reduce QW temperature.

Figure 6.29 compares a simulation with an external heat sink temperature of 300K for a structure with no "stub" and a structure with varying stub width. Figure 6.30 shows the corresponding LI curves. The inclusion of this stub decreases the QW temperature by a few Kelvin.

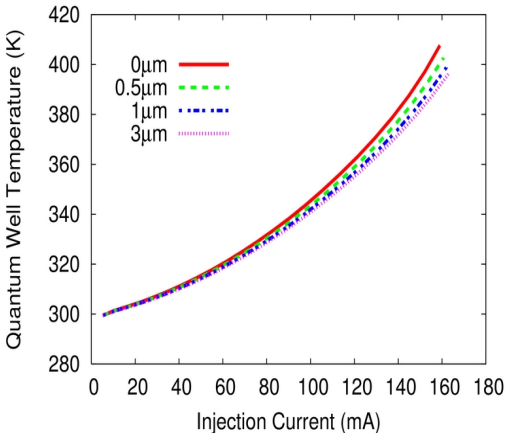

Figure 6.29: Introducing a small stub into the epitaxy to help reduce QW temperature.

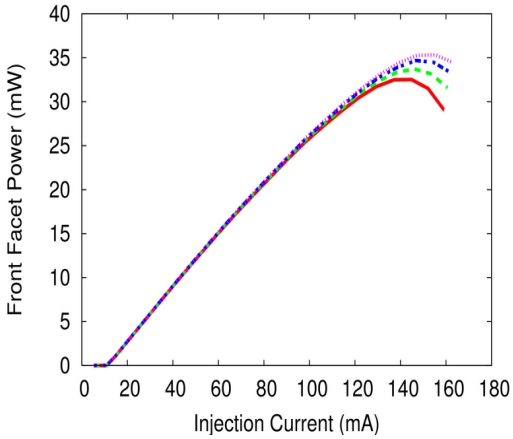

Figure 6.30: Introducing a small stub into the epitaxy pushes back the onset of roll-over.

Figure 6.31 plots the QW temperature as a function of injection current without a stub and with a stub of varying width at elevated temperatures of 360K. In the roll-over region, the stub decreases the QW temperature by up to 10K. However, in the normal operating region only a 3-5K decrease in QW temperature is observed. Figure 6.32 plots the corresponding LI curves, where a large change in the peak output power (~1mW) can be seen. However, it is not normal to run the device in this region, so it is probably not worth including the stub in real devices.

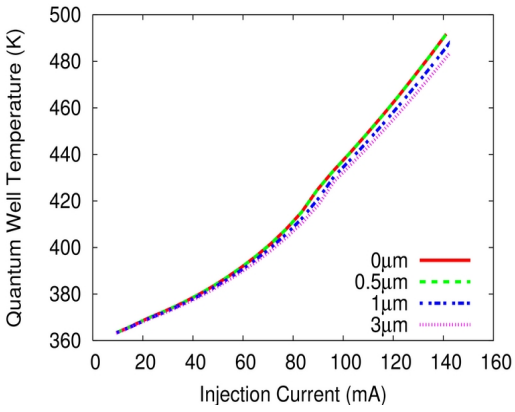

Figure 6.31: Introducing a small stub into the epitaxy to help reduce QW temperature at 360K

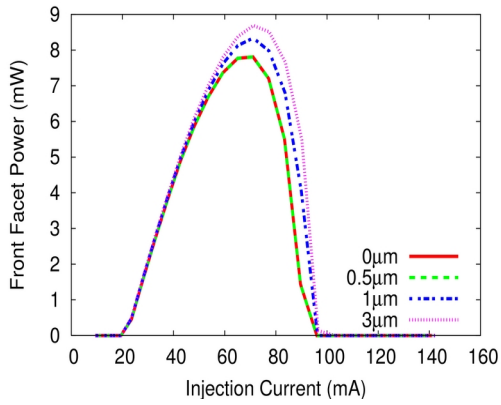

Figure 6.32: Introducing a small stub into the epitaxy pushes back the onset of roll-over at 360K

6.12 The effect of p-contact resistance

The specific contact resistance is defined as the measured contact resistivity times the area of the contact. The contact resistivity is defined as

$$\rho_c = \left.\frac{\partial J}{\partial V}\right|^{-1} (\Omega\, cm^2) \quad . \tag{6.1}$$

A very good contact resistivity is considered to be anything around $1x10^{-7}\Omega cm^2$, a poor contact resistivity is considered to be $1x10^{-5}\Omega cm^2$. In practice, anything below $1x10^{-6}\Omega cm^2$ is often considered acceptable for a modern semiconductor device. In a laser diode, a large p-contact resistance is particularly undesirable because of the closeness of the p-region to the active region, and the difficulty in removing heat from the ridge. A range of contact resistivity values were investigated to determine what

effect the contact resistance has on the device temperature. The results are shown in figures 6.33 and 6.34 for the devices processed for high and low modulation rates.

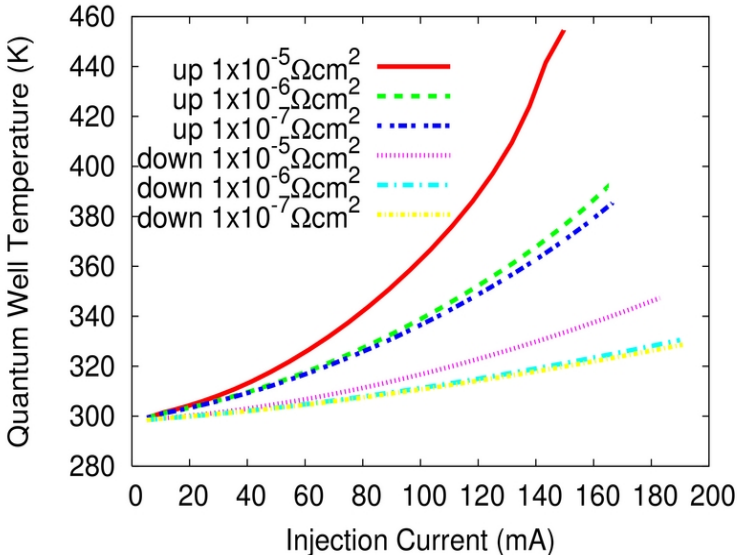

Figure 6.33: The impact of contact resistance on the device processed for a low modulation response.

It can be seen from figures 6.33 and 6.34 that the contact resistance has a larger impact on p-side up mounted devices than on p-side down mounted devices. This is because the contact resistance produces heat at the metal-semiconductor interface. Thus, in a p-side down mounted device, this heat source is closer to the heat sink, so that the heat generated by the contact resistance can quickly escape the device. A very poor contact resistance, i.e. $1x10^{-5}\Omega cm^2$, can produce a large increase in device heating (figure 6.33). The difference between a good ($1x10^{-6}\Omega cm^2$) and excellent ($1x10^{-7}\Omega cm^2$) contact resistance in terms of increased device temperature is small. Thus, as long as the contacts on the device are of relatively high quality, the heating due to the contact resistance should not be a major problem.

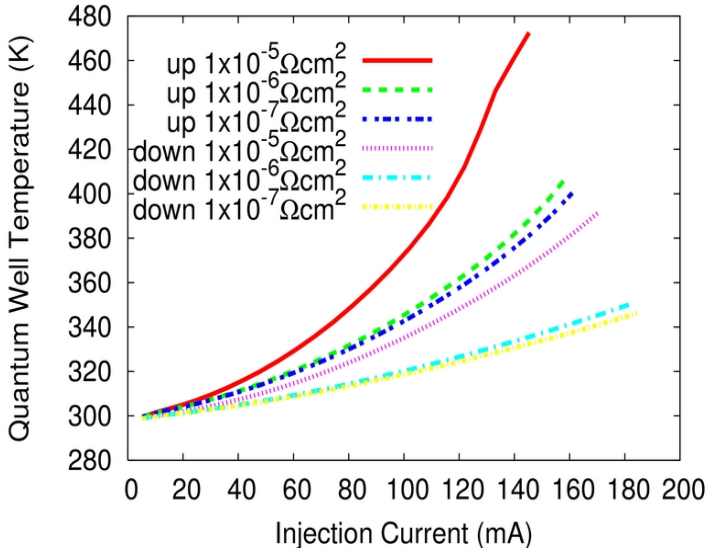

Figure 6.34: The impact of contact resistance on the device processed for a high modulation response.

6.13 Variation of ridge width

The ridge width is a critical device parameter. A narrow ridge results in a low threshold current and high maximum modulation rate. In figure 6.35, the quantum well temperature has been plotted as a function of injection current for ridge widths of 2µm, 3µm and 4µm. It can be seen that there is a thermal penalty for having a narrow ridge. There are two reasons for this. As the ridge narrows, the current density becomes higher, resulting in an increased rate of Joule heating and heating due to contact resistance. Secondly, a narrower ridge has a higher thermal resistance. Thus, any heat generated within the ridge will heat it up more. This is especially important in p-side up mounted devices, where there is a large thermal resistance between the bottom of the ridge and the heat sink. The corresponding LI curves are plotted in figure 6.36. Again, by mounting the device p-side down a considerable increase in performance can be gained. This performance improvement outweighs any gain from

variation of ridge width.

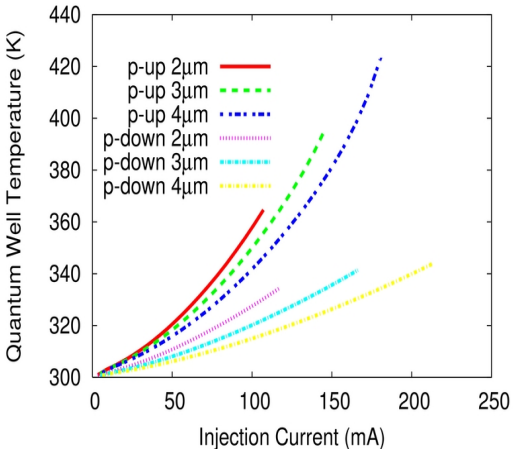

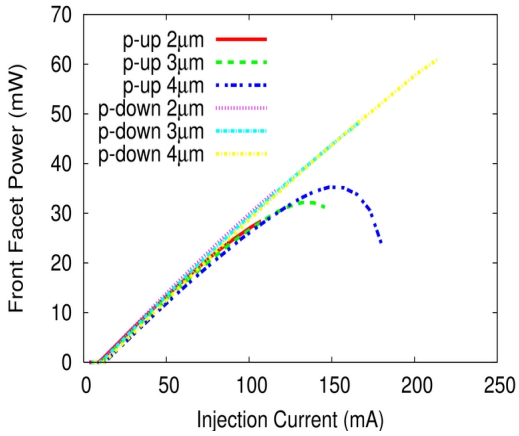

Figure 6.35: Injection current versus quantum well temperature for various ridge width.

Figure 6.36: LI curves for various ridge widths.

6.14 Optimisation of the doping of the p-type cladding

Heating in and around the ridge has been identified as an important issue, due to the difficulty of heat transport out of the active region in devices mounted p-side up. This makes it desirable to minimise the heat generated within the ridge. The two major heat sources within the RW are Joule heating and free carrier absorption (FCA). Far away from the QW where the photon density is low (e.g. at the top of the ridge), Joule heating plays an important role. To assess the impact of Joule heating, a plot of device resistance is shown in figure 6.37 for three different cladding doping levels - $1x10^{17}cm^{-3}$, $5x10^{17}cm^{-3}$ and $1x10^{18}cm^{-3}$. A doping level of $5x10^{17}cm^{-3}$ is the standard

doping used within the cladding of the 1.3μm devices. The graph was calculated by summing

$$\Delta R = \frac{\Delta x}{q(n\mu_n + p\mu_p)A} \tag{6.2}$$

during device operation, where ΔR is the resistance of a particular mesh point, Δx is the width of the calculation cell and A is the area of the p-contact. The p-contact is on the left of the graph and the substrate is on the far right side of the graph. The first major rise in device resistance on the left hand side of the graph is due to the low doping within the cladding region. The second major contributor to the device resistance comes from the GRIN layer. The reason for the high resistance of the GRIN layer is that it is left undoped to minimize FCA. As the doping concentration is increased within the cladding layer, not only does the resistance of the cladding decrease, but the resistance of the GRIN layer also decreases. This is because more holes diffuse from the cladding into the GRIN layer, increasing the carrier concentration and increasing the conductivity of the GRIN layers.

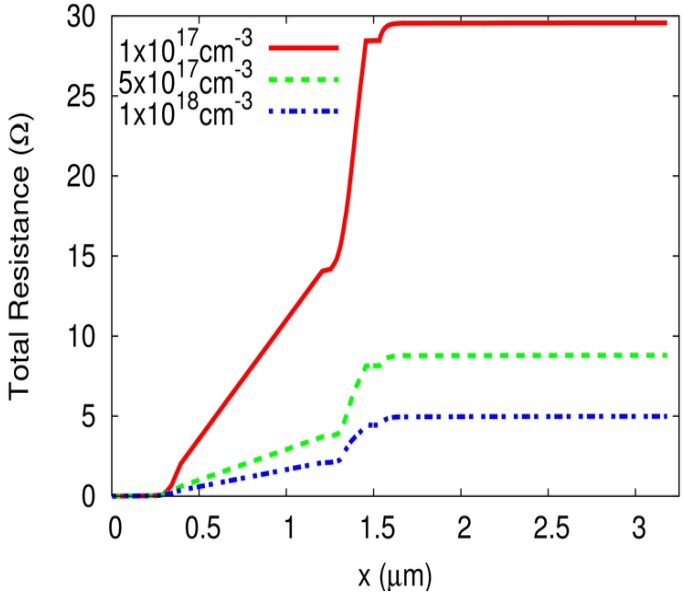

Figure 6.37: Plot of resistance throughout the device at 1.6V.

The original motivation for this work came from reasoning that the photon density is much higher close to the QW than further away from it. Thus, higher doping levels far from the QW should not really affect the FCA rate, so that the overall device resistance and Joule heating could be decreased. Before introducing graded doping into the cladding, the doping in the cladding region was optimized for a constant doping density. For an input power of 20mW and corresponding optical output of 5.5mW, a doping of $5x10^{17}cm^{-3}$ was found to be optimal. However, at an input power of 30mW giving an optical output power of around 9mW, a slightly higher doping of $7x10^{17}cm^{-3}$ was found to be optimal. The slightly higher optimum doping level is due to the increased heating causing a higher device temperature and thus lower mobility. Figure 6.38, shows the results of this investigation. The above investigation was performed with a 1D model as an initial investigation. A further and more comprehensive investigation can be found in [6].

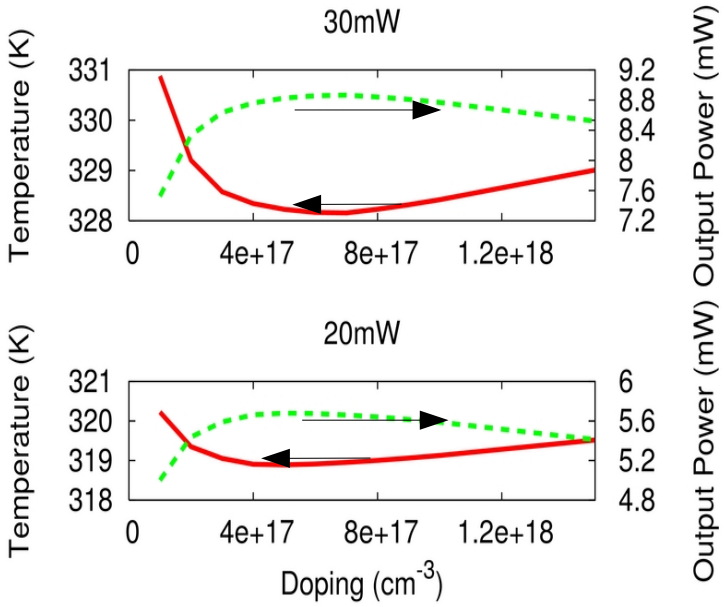

Figure 6.38: Quantum well temperature and front facet output power plotted at 20mW and 30mW of input power.

Error: Reference source not found6.15 Graded doping in the p-type cladding region

In order to minimise Joule heating and FCA, grading of the doping profile in the cladding region was investigated. At the contact, doping levels ranging from $1x10^{17}m^{-3}$-$1x10^{19}m^{-3}$ were investigated. The same values were also used to optimise the doping level closest to the QW. Thus, a square search was performed for the optimum linear cladding doping profile. An example of four doping profiles is depicted in figure 6.39.

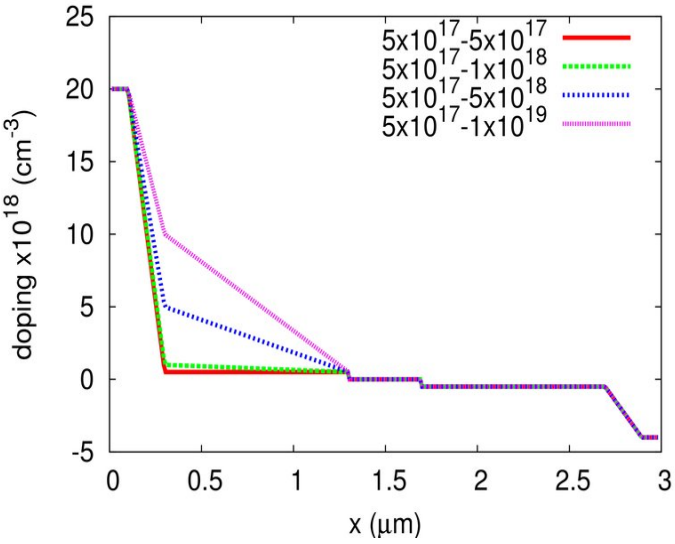

Figure 6.39: Graded doping profile, positive numbers indicate p-type doping, negative indicate n-type doping.

As would be expected, the doping profiles where the doping was higher closer to the QW proved not to be optimal because of the high level of FCA. A graded profile sloping downwards from the top contact to the QW proved to be the most effective in terms of maximum output power for minimum active region temperature. The results from this search are shown in figures 6.40 and 6.41 for heatsink temperatures of 300K and 360K, respectively. Only the original flat doping profile of $5x10^{17}m^{-3}$ and the other best results have been plotted in these figures for clarity. At 300K, the optimal graded doping profile is $1x10^{18}m^{-3}$ close to the quantum well and $5x10^{18}m^{-3}$ near the top contact. At 360K, the same doping profile was found to be optimal.

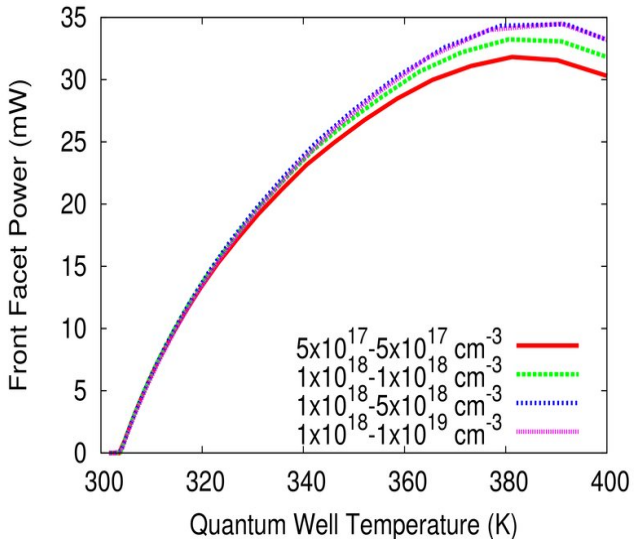

Figure 6.40: Front facet power plotted against quantum well temperature at 300K.

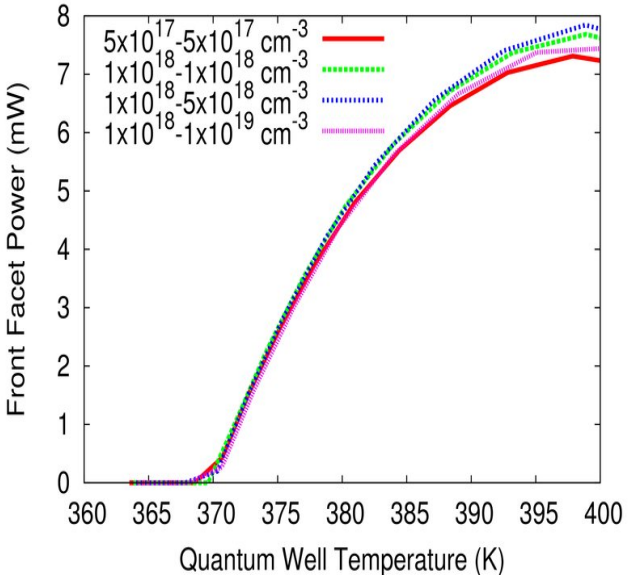

Figure 6.41: Front facet power plotted against quantum well temperature at 360K.

6.16 Summary

In this chapter, the simulation tool developed in Chapter 5 was used to optimise and investigate the design of the 1.3μm InGaAsN/GaAs double quantum well laser studied in Chapters 3 and 4. The following information has been learned during the course of this work:

1. The measured QW temperatures from Chapter 4 have been shown to give good agreement with the thermal model.
2. The thermal performance of the structure optimised for a high modulation rates has been shown to be inferior to that of the ordinary RW structure. This is because the ordinary RW structure has a high thermal conductivity layer of gold coating the ridge and etched trenches, whilst the mesa structure has a layer of low thermal conductivity BCB surrounding the ridge. In applications requiring only relatively low modulation rates (e.g. 1Gb/s up stream transmission from a home user to the optical network), it may be advantageous not to use the mesa structure to gain increased device lifetimes and reliability.
3. The thickness of the gold layer on the bottom of the etched trench of the ordinary RW structure has been shown to be an important device parameter - far more important than that around the ridge.
4. A wider ridge was found to reduce electrical resistance, thereby reducing the Joule heating. A wider ridge also decreases the thermal resistance. A wider ridge however increases threshold current and for a single-mode device there is also a limit to how wide the ridge can be.

5. P-side down mounting has been shown to be significantly better in terms of thermal performance than p-side up mounting. P-side down mounting is particularly beneficial for the large area mesa structure, due to its poor thermal performance.
6. Thinning the substrate has been shown to result in a significantly lower QW temperatures.
7. The depth of the etch down to the n-type substrate has been shown not to affect the thermal performance of the mesa structure.
8. Significant performance gains have been shown by using a more thermally conducting material when refilling the etched trenches. Refilling the etched trenches is technologically challenging. Therefore, connecting the top gold contact to the substrate with a stub was investigated. Whilst some benefits were seen, it was not as effective as replacing BCB with a more thermally conductive material.
9. The impact of contact resistance was investigated. It was found that while variation of contact quality from good to very good produces a small change in device temperature, it is probably not worth striving to achieve excellent contacts. In contrast, however, a poor contact resistance can dramatically push up the QW temperature.
10. The doping of the cladding region within the RW structure was optimised. It was found that a graded cladding region can be advantageous, by minimising both Joule and FCA throughout the RW.

P-side down mounting has shown the most impact on device temperature. If a low cost mount, capable of mounting the device p-side down whilst not adversely affecting the modulation response could be developed, this would be expected to significantly extend device lifetime.

6.17 References

[1] H. Ishikawa, T. Fujiwara, K. Fujiwara, M. Morimoto, and M. Takusagawa, "Accelerated aging test of $Ga_{1-x}Al_xAs$ DH lasers", 50 , 4, pp. 2518-2522, 1979

[2] J. Barry, A. Einhorn, G. Mecherle, P. Nelson, R. Dye and W . Archambeault, "Thermally accelerated life testing of single mode, double-heterostructure, AlGaAs laser diodes operated pulsed at 50mW peak power", IEEE J. Quant. Electron., 21, 4, pp. 365- 376, 1985

[3] W. Koechner, "Solid-State Laser Engineering", Springer Verlag, ISBN: 3540650644, pp. 329, 1999

[4] D. R. Lide, "CRC Hand book of Chemistry and physics 82nd edition", CRC press ,ISBN: 0849304822, 2001-2002

[5] A. Modafe, N. Ghalichechian, M. Powers, M. Khbeis and R. Ghodssi "Embedded benzocyclobutene in silicon: An integrated fabrication process for electrical and thermal isolation in MEMS" Microelectronic Engineering, 82, pp. 154–167, 2005

[6] R. MacKenzie, J.J. Lim, S. Bull, S. Sujecki and E.C. Larkins, "Inclusion of thermal boundary resistance in the simulation of high-power 980nm ridge waveguide

lasers", Submitted to Journal of Optical Quantum Electronics (Jan 07)